



This project has received funding from the European Union's Horizon 2020 research and innovation programme under grant agreement No. 700748

LIQUEFACT

Assessment and mitigation of Liquefaction potential across Europe: a holistic approach to protect structures/infrastructure for improved resilience to earthquake-induced Liquefaction disasters.

H2020-DRA-2015

GA no. 700748



DELIVERABLE D3.3

Design guidelines for the application of soil characterisation and liquefaction risk assessment protocols

Author(s):	António Viana da Fonseca, Maxim Millen, Xavier Romão, Julieth Quintero, Sara Rios and Abdelghani Meslem.
Responsible Partner:	University of Porto (UPorto)
Version:	1.0
Date:	31/12/2018
Distribution Level (CO, PU)	PU



This project has received funding from the European Union's Horizon 2020 research and innovation programme under grant agreement No. 700748

DOCUMENT REVISION HISTORY

Date	Version	Editor	Comments	Status
31/12/2018	1		First Draft	Draft

LIST OF PARTNERS

Participant	Name	Country
UPORTO	Universidade do Porto	Portugal
Istan-Uni	Istanbul Universitesi	Turkey
ULJ	Univerza V Ljubljani	Slovenia
UNINA	Universita degli Studi di Napoli Federico II	Italy
NORSAR	Stiftelsen Norsar	Norway
ARU	Anglia Ruskin University Higher Education Corporation	United Kingdom
UNIPV	Università degli Studi di Pavia	Italy
UNICAS	Universita degli Studi di Cassino e del Lazio Meridionale	Italy



This project has received funding from the European Union's Horizon 2020 research and innovation programme under grant agreement No. 700748

CONTENTS

EXECUTIVE SUMMARY.....	6
SCOPE AND PURPOSE	7
1. INTRODUCTION	8
2. CLASSIFICATION OF INFRASTRUCTURE AND SOIL DEPOSITS.....	9
2.1 KEY ASPECTS OF CLASSIFICATION OF INFRASTRUCTURE FOR LOSS AND RISK ASSESSMENT	9
2.2 KEY ASPECTS OF CLASSIFICATION OF LIQUEFACTION FOR LOSS AND RISK ASSESSMENT	10
2.3 CLASSIFICATION OF INFRASTRUCTURE	11
2.4 CLASSIFICATION OF SOIL PROFILE	14
REFERENCES.....	15
3. QUANTIFY THE SEISMIC HAZARD.....	17
REFERENCES.....	18
4. ASSESSMENT OF VULNERABILITY	19
4.1 THE EFFECTS OF LIQUEFACTION-INDUCED GROUND DEFORMATIONS ON THE PERFORMANCE OF BUILDINGS	20
4.2 METHODS TO QUANTIFY VULNERABILITY	22
4.3 DISCUSSION OF THE ROLE OF VULNERABILITY FUNCTIONS.....	23
REFERENCES.....	24
5. COMPUTATION OF LOSSES.....	26
5.1. LOSS CALCULATION EXAMPLE CASE STUDY	29
REFERENCES.....	33
6. FINAL REMARKS.....	34



This project has received funding from the European Union's Horizon 2020 research and innovation programme under grant agreement No. 700748

LIST OF FIGURES AND TABLES

FIGURES

Figure 2.1: Influence of liquefaction classification on uncertainty in fragility curves..... 11

Figure 2.2: Example of a building class from the GEM Building Taxonomy: attributes and associated levels of detail..... 12

Figure 2.3: The SERA project BCIM model - sources of uncertainty that have to be included in the derivation of vulnerability functions for a given building class where a limited number of attributes are known. 14

Figure 2.4: Liquefact soil profile classification criteria..... 14

Figure 2.5: Liquefact soil profile classes..... 15

Figure 4.1. Behaviour of frame buildings with flexible shallow foundations due to differential vertical ground settlements (Bird et al. 2006). 21

Figure 4.2. (a) Liquefaction-induced uniform vertical settlements of building with stiff shallow foundations; (b) differential vertical settlements of building (rotation) with stiff shallow foundations (Bird et al. 2006). 21

Figure 4.3: Dynamic performance parameters and residual performance parameters used to quantify the performance of a building. 22

Figure 4.4: Application of the macro-mechanism approach to assess vulnerability and losses..... 24

Figure 5.1: Obtaining probabilities from fragility curves 29



This project has received funding from the European Union's Horizon 2020 research and innovation programme under grant agreement No. 700748

TABLES

Table 2.1: Values of attributes of GEM Building Taxonomy used to describe European residential buildings 13

Table 5.1: Building damage states and associated losses and probabilities 30

Table 5.2: Foundation damage states and associated losses and probabilities 30

Table 5.3: Combine performance damage states and associated losses and probabilities 30

Table 5.4: Combined building foundation damage states 31

Table 5.5: Probabilities of each building-foundation damage state 31

Table 5.6: Losses associated to each building-soil damage state 32



This project has received funding from the European Union's Horizon 2020 research and innovation programme under grant agreement No. 700748

EXECUTIVE SUMMARY

This report provides an overview of the key steps for assessing the risk of infrastructures that are exposed to liquefaction and discusses key aspects related to the definition of exposure models (for infrastructures and soil deposits), seismic hazard, vulnerability assessment and expected loss quantification. Each topic is discussed in the context of liquefaction-induced ground deformations and their effect on the performance of buildings, highlighting the necessary requirements as well as the existing approaches and their limitations. Particular focus is given to features developed in LIQUEFACT. Among these, reference is made to the equivalent soil profile scheme for classifying liquefaction susceptibility for loss assessment and that should be combined with existing infrastructure taxonomies for the purpose of developing a combined exposure model accounting for liquefaction susceptibility. Likewise, reference is also made to a novel procedure presented for the calculation of losses accounting for liquefaction-induced ground deformations that is based on a state-of-the-art approach for calculating probabilistic losses from a seismic vulnerability assessment considering building, foundation and system damage states.



This project has received funding from the European Union's Horizon 2020 research and innovation programme under grant agreement No. 700748

SCOPE AND PURPOSE

This document provides an overview of the key steps for assessing the risk of infrastructure that are exposed to liquefaction. The main steps been classification of the soil deposit and the infrastructure of interest, quantify the seismic hazard, assess the vulnerability of the infrastructure, compute the expected losses. The document focuses on buildings, however, the discussion is applicable to other infrastructure (embankments, pipelines, bridges).

The first chapter provides a brief overview of probabilistic seismic risk assessment. The key attributes of exposure, hazard and vulnerability are covered.

The second chapter looks in detail at exposure and how to classify assets and soil liquefaction inside a loss assessment framework. The classification schema for buildings adopted in this project is explained. The equivalent soil profile scheme for classifying liquefaction susceptibility for loss assessment that was developed in LIQUEFACT D3.2 is briefly explained.

The third chapter focuses on seismic hazard, discussing the steps in quantifying seismic hazard. Recent advancements in seismic hazard quantification. The issues around multiple ground motion intensities measures are discussed, which is particularly relevant to soil-liquefaction-foundation-structure interaction problems where structural damage is typically best correlated to peak energy based intensity measures, while liquefaction is more strongly correlated to cumulative energy-based intensity measures.

Chapter 4 presents the keys steps in vulnerability assessment and reviews the vulnerability assessment procedure developed for assessing buildings on liquefiable soil deposits that was developed in LIQUEFACT Deliverable 3.2.

Chapter 5 focuses on the calculation of losses. A novel procedure is developed to combine conditioned fragility curves. A case study loss example calculation is presented that demonstrates how the exposure, hazard and vulnerability steps are used in the assessment of building losses.



This project has received funding from the European Union's Horizon 2020 research and innovation programme under grant agreement No. 700748

1. INTRODUCTION

Probabilistic seismic risk and loss assessment involves the estimation of the probability of damage and losses resulting from potential future earthquakes. This damage and loss might occur to buildings, infrastructure, people or even the environment. The risk/loss framework that is being developed by LIQUEFACT is applicable for estimating damage and loss in built infrastructures such as residential, commercial and industrial buildings. A probabilistic seismic risk and loss assessment will perform the calculation and convolution of seismic hazard, vulnerability functions for the elements at risk, and the exposure model describing primarily the location and value of the elements at risk, **Equation (1.1)**.

$$SEISMIC\ RISK = SEISMIC\ HAZARD \otimes VULNERABILITY \otimes EXPOSURE \quad (1.1)$$

To perform a probabilistic seismic risk and loss assessment at the regional level, the elements at risk (i.e. the built infrastructure) need to be formally clustered according to building classes which are then organized using a spatial inventory system defining the exposure model. Vulnerability functions will therefore need to be defined for each building class and seismic hazard needs to be mapped at a scale compatible with the regional level assessment that needs to be performed. On the contrary, for a building-specific seismic risk and loss assessment, there is no need for a formal exposure model (i.e. the exposure term of **Equation (1.1)** becomes 1), the necessary vulnerability functions are also building-specific and the seismic hazard needs to be that of the location of the building.



This project has received funding from the European Union's Horizon 2020 research and innovation programme under grant agreement No. 700748

2. CLASSIFICATION OF INFRASTRUCTURE AND SOIL DEPOSITS

Most of the aspects related to the classification of infrastructures discussed in this section are solely relevant for performing a probabilistic seismic risk and loss assessment at the regional level, given the level of uncertainty about the real characteristics of those infrastructures. For a building-specific seismic risk and loss assessment, it is expected that adequate and detailed information about the necessary characteristics of the building is available or can be obtained based on detailed surveys of the building. The case study building presented in the LIQUEFACT report D3.2 section 2.8 (Viana da Fonseca et al., 2018), presents the classification of a single building, while the classification of an embankment class is shown in case study D3.2 chapter 3 (Viana da Fonseca et al., 2018).

2.1 KEY ASPECTS OF CLASSIFICATION OF INFRASTRUCTURE FOR LOSS AND RISK ASSESSMENT

For performing a probabilistic seismic risk and loss assessment at a regional level, an exposure model of the elements at risk needs to be developed. To ensure a full compatibility between the exposure model and the fragility/vulnerability functions, it is necessary to classify these elements using a common language or classification scheme, i.e. a taxonomy. The main classifications of European residential buildings that were used in past risk assessment research and projects (e.g. RISK-UE, LESSLOSS) were reviewed in the European FP7 research project NERA (Network of European Research Infrastructures for Earthquake Risk Assessment and Mitigation) (Crowley et al., 2015). These classes of buildings were typically described with a simple classification scheme (e.g. RC1L refers to low-rise reinforced concrete moment frames) that was not easy to expand in order to include missing types of construction, such as those used for commercial and industrial buildings. They did not make use of a comprehensive building taxonomy. To address this lack of flexibility, the NERA project used the GEM Building Taxonomy (Brzev et al., 2013) to classify European residential buildings.

The GEM Building Taxonomy is a uniform classification system supported by the Global Earthquake Model (www.globalquakemodel.org) that can be applied to buildings across the globe. A genetic code (genome) that is a unique description for a building or a building typology can be generated using this taxonomy. This code is defined by 13 main attributes and each attribute corresponds to a specific building characteristic that affects its seismic performance such as material, lateral load-resisting system, building height, etc. The taxonomy is organized as a series of expandable tables and each attribute can be described by one or more level of detail (**Figure 2.2**). The main benefit of the GEM Building Taxonomy is that it is expandable and collapsible, and so it can be used to describe both the detailed attributes of a single building as well as the general characteristics of a structural system used for a class of buildings. It is thus ideal for a risk framework that should lay out the principles of damage and loss assessment for different scales of resolution, from site-specific, to local, to national/continental (often also referred to as regional). Many of the attributes in the taxonomy are also relevant for other natural hazards, and expansion of the taxonomy for use in flood, storms



This project has received funding from the European Union's Horizon 2020 research and innovation programme under grant agreement No. 700748

and volcano risk is being carried out in collaboration with the World Bank's Global Facility for Disaster Risk Reduction (GFDRR), the CIMA Foundation (International Centre on Environmental Modelling), and the British Geological Survey.

A few attributes of the GEM building taxonomy are currently being modified and expanded for the purpose of the European risk framework under development by the European H2020 research project SERA (Seismology and Earthquake Engineering Research Infrastructure Alliance for Europe) (<http://www.sera-eu.org>) for residential, commercial and industrial buildings. Among other aspects that have been identified as requiring further developments (Crowley et al., 2017), reference is made to the classification of the ductility of lateral load resisting systems and of the foundation systems. For example, the former should include an attribute of the level of ductility enforced by the design code used at the time of construction while the latter should be expanded to account for the foundation soil type in order to allow the soil-structure interaction effects.

2.2 KEY ASPECTS OF CLASSIFICATION OF LIQUEFACTION FOR LOSS AND RISK ASSESSMENT

A similar framework to the GEM framework for buildings was developed in LIQUEFACT Deliverable 3.2 for classification of liquefaction potential for soil deposits (Viana da Fonseca et al., 2018). The classification uses just three attributes, cyclic resistance, depth and height of a critical liquefiable layer. The attributes and criteria for the classes were chosen to best capture the performance of a building on a liquefiable soil deposit (Millen et al. 2019), but can be applied to other infrastructure such as embankments (see chapter 3 in Viana da Fonseca et al., 2018). This classification scheme provides a simple extension to the building classification to make a building-soil-profile classification.

Although the equivalent soil profile has physically measurable parameters, the classification system was developed to quantify performance. The focus on performance is important since liquefaction can be both beneficial to building performance (reduced seismic action) and detrimental (increased settlement and tilt). If the classification system failed to isolate the beneficial and detrimental effects than the fragility curves that would be developed would represent high levels of uncertainty (**Figure 2.1** - right) since there would be a large variation in performance. Whereas, optimal classification would clearly distinguish the behaviour of different classes ((**Figure 2.1** – left, Liq class 1 – liquefaction is detrimental, Liq class 2 – liquefaction is beneficial).

The combination of the building and soil classes allows the influence of settlement, tilt, soil-foundation impedance and dynamic site response to implicitly be accounted for in the performance of the building. Alternative procedures such as Bird et al. (2006) consider liquefaction effects based on liquefaction intensity measures (e.g. Liquefaction Severity Number (LSN) (Van Ballegooy 2015)) and require interaction factors or utility functions between shaking damage and liquefaction damage to calculate the overall performance. The development of interaction factors is non-trivial as the quantification of the major aspects of soil-structure interaction is dependent on the position and height of the liquefiable layer, as well as the time at which liquefaction occurs during a shaking event (Millen et al., 2019). These attributes are not explicitly considered



This project has received funding from the European Union's Horizon 2020 research and innovation programme under grant agreement No. 700748

in singular intensity measures and therefore large uncertainty in the performance can be expected. Alternatively, assessment of liquefaction risk requires comparison of the anticipated level of loading (i.e. earthquake-induced ground shaking) imposed on a soil deposit with the inherent resistance of the soil to liquefaction. Since both loading and resistance can vary with depth, the potential for liquefaction must be evaluated at different depths within the soil profile of interest.

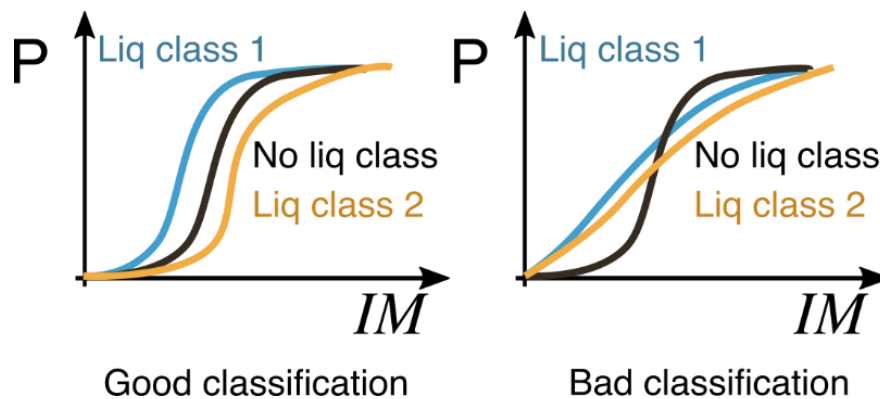


Figure 2.1: Influence of liquefaction classification on uncertainty in fragility curves

2.3 CLASSIFICATION OF INFRASTRUCTURE

As referred by (Crowley et al., 2018), various building inventory databases have been developed at a global scale, following different approaches and with distinct levels of accuracy and reliability. For example, Jaiswal et al. (2010) developed a global building inventory database for the PAGER system, which provides a distribution of building classes for urban and rural areas, at a national scale. This database harmonizes various sources of information and applies mapping schemes to infer structural building types globally. This database is open and publicly available. Another example is the Global Exposure Database (GED) from the Global Earthquake Model (GEM) that provides a spatial inventory of residential buildings and population for the purposes of seismic risk modelling and earthquake loss estimation (Gamba, 2014). Data is available at three different geographical scales and the sources of information depend on the selected scale. The datasets used to populate GED include the Database of Global Administrative Areas (GADM), the Global Rural-Urban Mapping Project (GRUMP), the Gridded Population of the World (GPW), the Multiple Indicator Cluster Surveys (MICS), UN Habitat's Global Urban Observatory (GUO) data, United Nations statistics, PAGER building inventory database, among others. The GED database is publicly available through the OpenQuake platform. Another global initiative regarding building inventories is The World Housing Encyclopedia (WHE, 2014). Detailed housing reports from all over the world are publicly available and include information about the building type, construction practice, average floor areas, average construction cost, and a qualitative estimation of building's vulnerability under seismic events. However, the WHE reports do not cover the number of buildings in each country or the associated geographical distribution.



This project has received funding from the European Union's Horizon 2020 research and innovation programme under grant agreement No. 700748

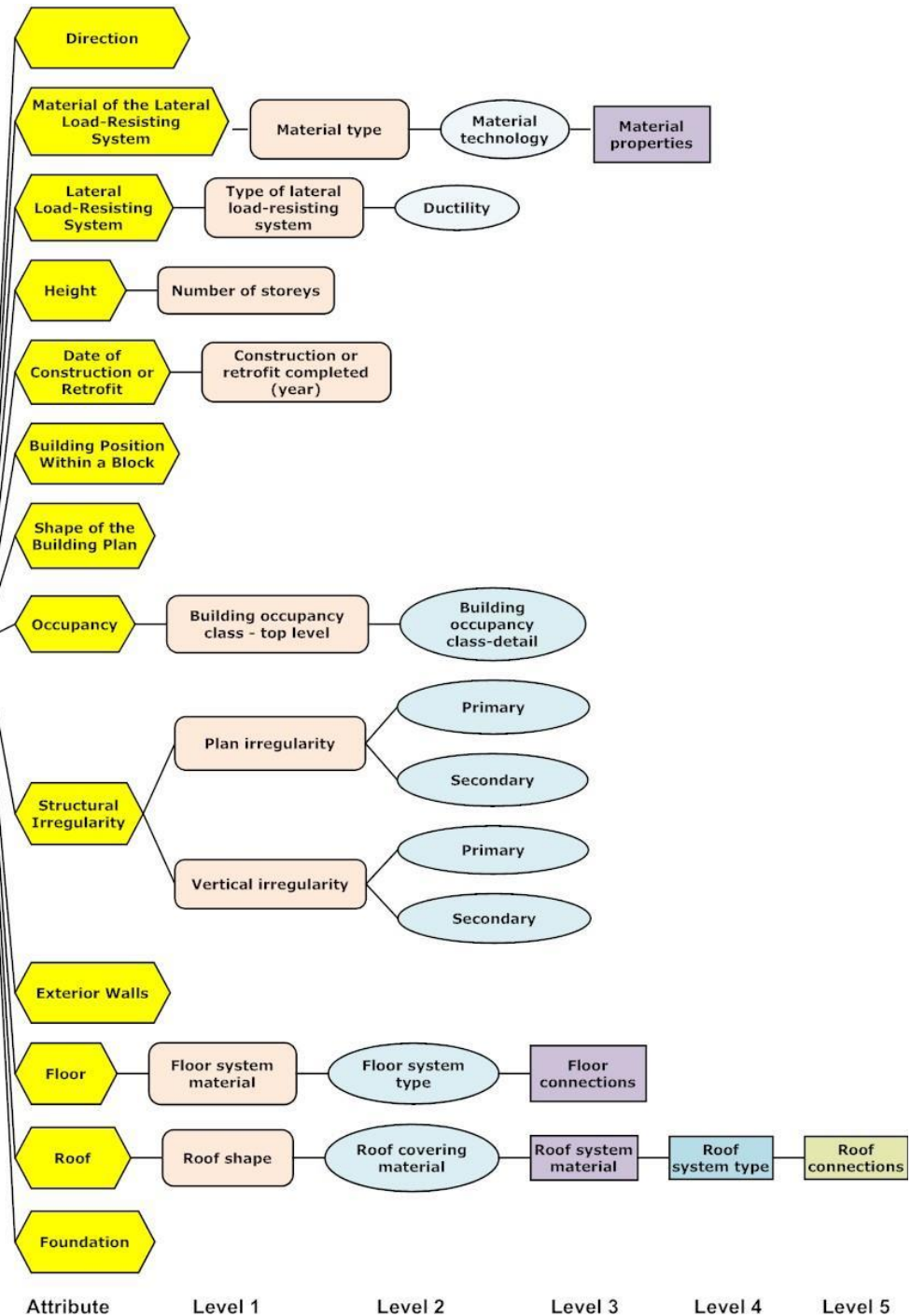


Figure 2.2: Example of a building class from the GEM Building Taxonomy: attributes and associated levels of detail

Currently, as part of the European risk framework work package of the H2020 SERA project, further efforts are being made to collect the latest building and population/dwelling census data across Europe at the smallest possible administrative level, to involve structural engineers from a number of countries across



This project has received funding from the European Union's Horizon 2020 research and innovation programme under grant agreement No. 700748

Design guidelines for the application of soil characterisation and liquefaction risk

Europe in the development of the mapping schemes for residential buildings, and to further improve different aspects of the NERA methodology. The development of the European residential exposure model of the SERA project follows four main steps: i) definition of building classes, ii) mapping census data to building classes, iii) mapping dwellings to building, and iv) estimation of replacement cost and number of occupants. The starting point of the exposure model under development within SERA considers the attributes presented in **Table 2.1** as characteristics that can be assessed at a regional scale. In addition to these attribute values, two additional values are expected to be included in the final version of the SERA exposure model. These two additional values will address the characteristics of the structural design of the building (which will reflect the expected level of ductility of the structure) and the level of the design seismic action.

Table 2.1: Values of attributes of GEM Building Taxonomy used to describe European residential buildings

ATTRIBUTE	CODE	LEVEL 1 VALUE	CODE	LEVEL 2 VALUE
MATERIAL OF LATERAL LOAD-RESISTING SYSTEM	CR	Concrete, reinforced	PC	Precast concrete
	MUR	Masonry, unreinforced	CB99	Concrete blocks, unknown type
	MR	Masonry, reinforced	CL99	Fired clay unit, unknown type
	MCF	Masonry, confined	ST99	Stone, unknown technology
	MATO	Material, other	ADO	Adobe blocks
	ER	Earth, reinforced		
	W	Wood		
LATERAL LOAD-RESISTING SYSTEM	S	Steel		
	LWAL	Wall	DUCL	Ductile, low
	LDUAL	Dual frame-wall	DUCM	Ductile, medium
	LFM	Moment frame	DUCH	Ductile, high
HEIGHT	H	Number of storeys above ground	DN	Non-ductile
			HBET	Range
			HEX	Exact number

The fragility/vulnerability functions of buildings classes are seen to depend on these collectable attributes and their values. Still, these fragility/vulnerability functions also depend on information about other building characteristics that are difficult or even impossible to collect at a regional scale. Among other aspects of the risk framework under development by the SERA project, one of its key aspects is the ability to be able to incorporate sources of uncertainty associated to the building class coming from attributes that are not explicitly characterized. Since these additional attributes are unknown, building classes defined based on available information (i.e. information that can be collected) can be seen as *condensed* building classes that need to be *unfolded* so the contribution to the seismic vulnerability of the building class of the remaining unknown attributes can be characterized. The association of these unfolded building class attributes with the



This project has received funding from the European Union's Horizon 2020 research and innovation programme under grant agreement No. 700748

Design guidelines for the application of soil characterisation and liquefaction risk

information about the known attributes defines a Building Class Information Model (BCIM). The development of the BCIM of a given building class is currently being carried out within the SERA project and will be able to include the necessary information to compute the total variability of the fragility/vulnerability function associated to that building class. Therefore, the BCIM can be integrated with the seismic risk and loss framework developed by LIQUEFACT. The main aspects of the BCIM in terms of the relevant sources of uncertainty due to attributes that are not explicitly characterized are illustrated in **Figure 2.3**.

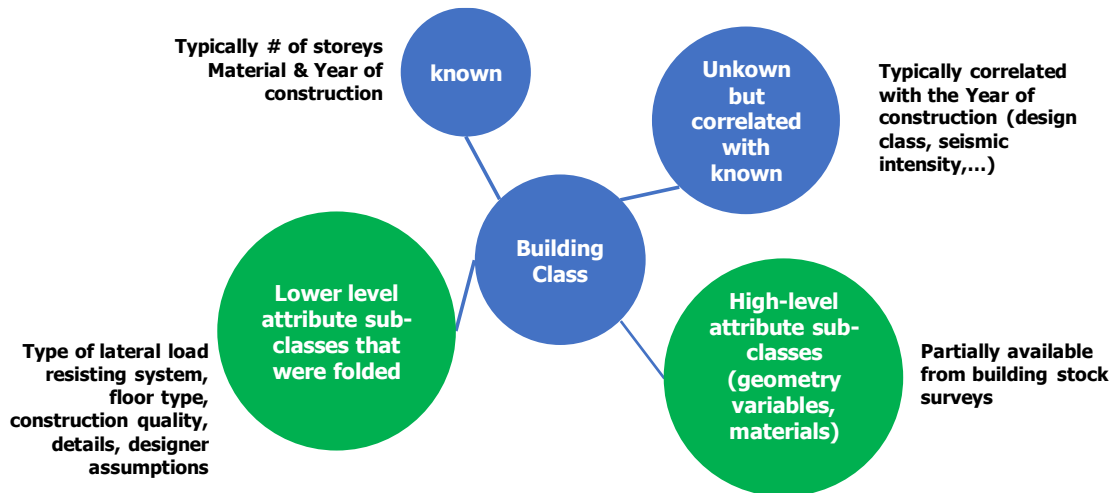


Figure 2.3: The SERA project BCIM model - sources of uncertainty that have to be included in the derivation of vulnerability functions for a given building class where a limited number of attributes are known.

2.4 CLASSIFICATION OF SOIL PROFILE

The LIQUEFACT soil profile classification criteria are outlined in **Figure 2.4** and produce the 22 classes in **Figure 2.5** using that criteria. A soil profile can either be classified using CPT, SPT, DMT, Vs logging or laboratory data for a building specific study, or taken for macro-zonation maps using the procedures outlined in section 2.3 of Deliverable 3.2 (Viana da Fonseca et al., 2018).

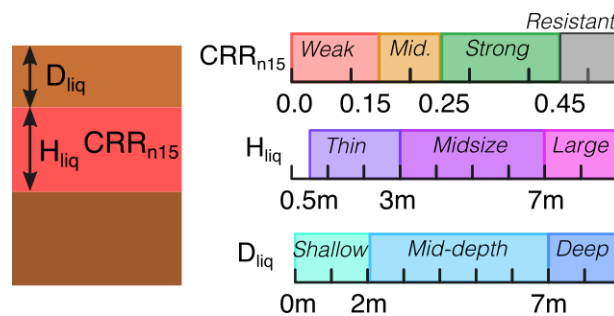


Figure 2.4: Liquefact soil profile classification criteria



This project has received funding from the European Union's Horizon 2020 research and innovation programme under grant agreement No. 700748

Design guidelines for the application of soil characterisation and liquefaction risk assessment protocols

Strength - Size - Position

		Weak	Mid.	Strong	Resist
Large	Shallow	WLS	MLS	SLX	RXX
	Mid.	WLM	MLM		
	Deep	WLD	MLD		
Midsize	Shallow	WMS	MMS	SMX	
	Mid.	WMM	MMM		
	Deep	WMD	MMD		
Thin	Shallow	WTS	MTS	STX	
	Mid.	WTM	MTM		
	Deep	WTD	MTD		

Figure 2.5: Liquefact soil profile classes

The additional unclassified attributes for the soil profile, e.g. shear modulus, void ratio, permeability should be obtained either directly through laboratory or field tests and correlations in literature for building specific studies. Or for regional scale behaviour the values should be sampled through correlations that are consistent with cyclic resistance, soil behaviour index and effective stress.

REFERENCES

Bird, J.F., Bommer, J.J., Crowley, H. and Pinho, R. (2006) Modelling liquefaction-induced building damage in earthquake loss estimation. *Soil Dynamics and Earthquake Engineering* 26(1), 15–30.

Brzev S., Scawthorn, C., Charleson, A., Allen, L., Greene, M., Jaiswal, K. and Silva, V. (2013), GEM Building Taxonomy Version 2.0. GEM Technical Report 2013-02 V1.0.0, 182 pp., GEM Foundation, Pavia, Italy, DOI: 10.13117/GEM.EXP-MOD.TR2013.02. Available from URL: <https://www.globalquakemodel.org/single-post/2017/05/17/GEM-Building-Taxonomy-Version-20>

BU-KOERI (2010) Earthquake loss estimation routine-ELER v3.0, Technical manual

Crowley H. Özcebe S., Spence R., Foulser-Piggott R., Erdik M. and Alten K.(2012) Development of a European Building Inventory Database. Proceedings of 15th World Conference on Earthquake Engineering, Lisbon, Portugal.

Crowley H., Colombi M. and Ozcebe S. (2015) D7.3 European Building Classification. NERA Deliverable 7.3, available from: https://www.orfeus-eu.org/other/projects/nera/NERA_D7.3.pdf

Crowley, H., Despotaki, V., Silva, V., Ptilakis, D., Ptilakis, K., Hancilar, U., Bursi, O., Wenzel, M., di Filippo, R. and Castro, J. (2017) D26.1 Taxonomy of European residential, commercial, industrial buildings and industrial plants. SERA Deliverable 26.1. Seismology and Earthquake Engineering Research Infrastructure Alliance for Europe.

Crowley, H., Rodrigues, D., Despotaki, V., Silva, V., Covi, P., Ptilakis, K., Ptilakis, D., Riga, E., Karatzetzou, A., Romão, X., Castro, J., Pereira, N. and Hancilar, U. (2018) D26.2 Methods for Developing European Residential Exposure Models. SERA Deliverable 26.1. Seismology and Earthquake Engineering Research Infrastructure Alliance for Europe.

Gamba, P. (2014) Global Exposure Database: Scientific Features, GEM Technical Report 2014-10 V1.0.0, 46 pp., GEM Foundation, Pavia, Italy, doi: 10.13117/GEM.EXP-MOD.TR2014.10.

Jaiswal, K. and Wald, D. (2008) Creating a global building inventory for earthquake loss assessment and risk management, U.S. Geological Survey Open-File Report-1160.

Jaiswal, K., Wald, D., and Porter, K. (2010) A Global Building Inventory for Earthquake Loss Estimation and Risk Management, *Earthquake Spectra*, 26(3), 731–748.



This project has received funding from the European Union's Horizon 2020 research and innovation programme under grant agreement No. 700748

LIQUEFACT
Deliverable D3.3
Design guidelines for the application of soil characterisation and liquefaction risk
assessment protocols
v. 1.0

- Viana da Fonseca, A., Millen, M., Romão, X., Quintero, J., Rios, S., Ferreira, C., Panico, F., Azeredo, C., Pereira, N., Logar, J., Oblak, A., Dolšek, M., Kosič, M., Kuder, S., Logar, M., Oztoprak, S., Kelesoglu, M. K., Sargin, S., Oser, C., Bozbey, I., Flora, A., Billota, E., Protá, A., Di Ludovico, M., Chiaradonna, A., Modoni, G., Paoletta, L., Spacagna, R., Lai, C.G., Shinde, S. and Bozzoni, F. (2018). Methodology for the liquefaction fragility analysis of critical structures and infrastructures: description and case studies. DELIVERABLE 3.2 of LIQUEFACT project "Assessment and mitigation of liquefaction potential across Europe: a holistic approach to protect structures / infrastructures for improved resilience to earthquake-induced liquefaction disasters" (www.liquefact.eu)
- Millen, M., Ferreira, C., Quintero, J., Gerace, A. and Viana da Fonseca, A. (2019). Simplified equivalent soil profiles based on liquefaction performance. 7th International Conference on Earthquake Geotechnical Engineering. Rome, Italy.
- Van Ballegooy, S., Wentz, F. and Boulanger Ross (2015). Evaluation of CPT-based Liquefaction Procedures at Regional Scale. Soil Dynamics and Earthquake Engineering.
- WHE (2014) Housing Reports. World Housing Encyclopedia, available at <http://db.world-housing.net/>



This project has received funding from the European Union's Horizon 2020 research and innovation programme under grant agreement No. 700748

3. QUANTIFY THE SEISMIC HAZARD

Typically, hazard is defined in terms some ground motion intensity measure (IM) versus return period. The choice of IM has a large impact on the level of uncertainty in the loss assessment (Luco and Cornell, 2007).

The recent study by Dashti and Karimi (2017) analysed the performance of different IMs on the liquefaction hazard in the far-field and near shallow-founded structures, expressing liquefaction hazard in terms of peak excess pore pressure ratio. The detailed study involved solid-fluid, fully-coupled, 3D nonlinear, dynamic finite element simulations of structures founded on a layered soil profile, including a liquefiable layer, accounting for the excess pore pressure redistribution and soil-structure interaction when evaluating the liquefaction hazard and effects on structures. Results from this study indicate that the best IMs, in terms of efficiency, sufficiency, and predictability, to estimate the peak excess pore pressure ratio are the spectral acceleration at the fundamental period of the site (for far-field prediction), peak ground acceleration (for predictions at the centre of a shallow foundation) and Arias Intensity (for predictions at the edge of a shallow foundation). A companion study more focussed on estimating the performance of shallow-founded structures (Karimi and Dashti, 2017) following the same detailed numerical approach concluded that IMs based on cumulative absolute velocity (CAV) have significant potential to estimate some of the relevant response parameters. However, even though such measures seem to have adequate characteristics in terms of efficiency, sufficiency, and predictability for ground settlements, IMs based on spectral acceleration at a given period still exhibit a better performance to represent structural response in terms of interstorey drifts (Karimi and Dashti, 2017). Estimates of cumulative permanent settlements of structures are expected to be influenced by the intensity, duration, and frequency content of the ground motion applied to the to the soil-structure system, thus indicating they should correlate well with IMs such as CAV which is evolutionary with time. On the other hand, peak values of interstorey drift in structures (which is not a cumulative demand parameter) was, is expected to better correlate with IMs that quantify seismic intensity and frequency content, as opposed to duration. As can be anticipated, this dichotomy casts several issues regarding the best approach for ground motion selection in a situation where both types of response measures may be relevant.

Notwithstanding this issue, the selection of the most adequate IM for representing peak structural response in situations where liquefaction or soil-structure interaction are not relevant is still an open debate. Kostinakis et al. (2018) recently presented a review of several scalar IMs and concluded that no specific IM is appropriate for all structures regardless of their features. Although they also address more advanced IMs, such as those dedicated to the simulation of spatially distributed structures, they did not analyse a new measure that is being increasingly used in regional risk assessments and that is planned to be used as one of the IMs for the fragility/vulnerability models developed by the SERA project. This measure is the average spectral acceleration, $avgSa$, defined as the mean of the log spectral accelerations at a set of periods of interest (Kazantzi and Vamvatsikos, 2015):

$$avgSa = \frac{1}{N} \sum_{i=1}^N \ln Sa(c_i \times T_i) \quad (3.1)$$



This project has received funding from the European Union's Horizon 2020 research and innovation programme under grant agreement No. 700748

where N is the number of periods used to compute $avgSa$ and the c_i terms are non-negative values to represent the range of selected periods as a function of the 1st mode period T_1 (e.g. $0.2 \cdot T_1$ to $3 \cdot T_1$ with a uniform period spacing of 0.01 s). This IM has been shown to be predicted with less uncertainty from the ground motion prediction equation perspective, to be an efficient predictor of structural response and to be sufficient with respect to ground motion properties affecting structural response (e.g. see (Eads et al., 2015, Kazantzi and Vamvatsikos, 2015)). Following the development of this IM, a conditional spectrum (CS) record selection method based on $avgSA$ was recently proposed (Kohrangi et al., 2018) that ensures an increased efficiency and sufficiency in simultaneously estimating multiple structural response parameters using this IM.

Furthermore, recent research by Millen et al. (2019) presented a closed form solution for the cumulative absolute strain energy (CASE) that was also shown to be an ideal candidate for assessing the triggering of liquefaction. The closed form solution makes use of the nodal surface energy spectrum (NSES) and Millen et al. (2019) proposes that the average of the NSES at the times corresponding to two times the shear wave travel time from the surface would represent the optimal intensity measure for ground motion selection. Unfortunately, no ground motion prediction equations exist for this parameter and therefore further research is needed before it can be used for this purpose. However, the parameter scales to the power of two as the amplitude scales, whereas intensity measures for superstructure damage (e.g. $avSa$) scale proportional to amplitude. Therefore, scaling ground motions for superstructure damage causes a bias with respect to the demand experienced by soil for liquefaction assessment.

Going back to the issue where estimates of both peak and cumulative demand parameters are required, it is noted that the generalized conditional intensity measure (GCIM) approach proposed by Bradley (2010) could be used to achieve a better correlation for cumulative demand parameters. The GCIM is a generalization of the CS method for cases where non-spectral ground motion IMs (e.g. record duration or Arias Intensity) are important to the prediction of structural response. The focus of CS is on improving the sufficiency with respect to spectral shape, while the GCIM enlarges this focus by seeking a sufficiency improvement with respect to other ground motion characteristics that are relevant to the response.

REFERENCES

- Bradley B.A. (2010) A generalized conditional intensity measure approach and holistic ground-motion selection. *Earthquake Engineering and Structural Dynamics*; 39(12), 1321–1342.
- Cornell C.A. and Krawinkler H (2000). Progress and challenges in seismic performance assessment, *PEER Centre News* 3(2):1-3.
- Dashti, S. and Karimi, Z. (2017) Ground motion intensity measures to evaluate I: the liquefaction hazard in the vicinity of shallow-founded structures. *Earthquake Spectra*, 33(1), 241-276.
- Eads, L., Miranda, E. and Lignos, D. G. (2015) Average spectral acceleration as an intensity measure for collapse risk assessment. *Earthquake Engineering & Structural Dynamics*, 44(12), 2057-2073.
- Karimi, Z. and Dashti, S. (2017) Ground motion intensity measures to evaluate II: the performance of shallow-founded structures on liquefiable ground. *Earthquake Spectra*, 33(1), 277-298.
- Kazantzi, A. K. and Vamvatsikos, D. (2015) Intensity measure selection for vulnerability studies of building classes. *Earthquake Engineering & Structural Dynamics*, 44(15), 2677-2694.



This project has received funding from the European Union's Horizon 2020 research and innovation programme under grant agreement No. 700748

- Kohrangi, M., Bazzurro, P., Vamvatsikos, D. and Spillatura, A. (2018) Conditional spectrum based ground motion record selection using average spectral acceleration. *Earthquake Engineering & Structural Dynamics*, 47(1), 265-265.
- Kostinakis, K., Fontara, I. K. and Athanatopoulou, A. M. (2018) Scalar structure-specific ground motion intensity measures for assessing the seismic performance of structures: a review. *Journal of Earthquake Engineering*, 22(4), 630-665.
- Luco, N., and Cornell, C. A. (2007) Structure-specific scalar intensity measures for near-source and ordinary earthquake ground motions. *Earthq Spectra* 23:357–392
- Millen, M., Ferreira, C., Quintero, J., Gerace, A. and Viana da Fonseca, A. (2019). Simplified equivalent soil profiles based on liquefaction performance. 7th International Conference on Earthquake Geotechnical Engineering. Rome, Italy.

4. ASSESSMENT OF VULNERABILITY



This project has received funding from the European Union's Horizon 2020 research and innovation programme under grant agreement No. 700748

4.1 THE EFFECTS OF LIQUEFACTION-INDUCED GROUND DEFORMATIONS ON THE PERFORMANCE OF BUILDINGS

The LIQUEFACT D3.1 report by Viana da Fonseca et al. (2017) addressed the most influential liquefaction-induced mechanisms relevant to the performance of buildings, including the initiation of liquefaction in the free-field, the influence of the building on the initiation of liquefaction, the dynamic response of the soil, the dynamic response of the structure and the structural damage mechanisms. The influence of liquefaction was quantified into three aspects, permanent deformations, modification to seismic energy entering the building, and modification to the soil-foundation impedance. The influence of all three aspects were directly tied to the equivalent soil profile classification developed in Liquefact Deliverable 3.2 section 2.3 (Viana da Fonseca et al., 2018), while the permanent deformation and in soil-foundation impedance are also strongly related to the geometry, foundation and load of the building. The modification to ground surface acceleration due to liquefaction is explored in section 2.7 (Viana da Fonseca et al., 2018), the influence on settlements and tilt is explored in section 2.6 (Viana da Fonseca et al., 2018) and the influence on soil-foundation impedance is discussed in section 2.2 (Viana da Fonseca et al., 2018).

The performance of a building is typically quantified in terms of collapse peak and residual inter-storey drift. However, due to the significant damage at the foundation that can occur due to liquefaction, the foundation tilt should also be considered as an additional performance parameter to capture the overall performance. The foundation tilt can either be global tilt, difference in vertical displacement across the length of the building divided by the length, or local foundation deformation, the vertical difference between two adjacent footings divided by the distance between them. The magnitude and type of foundation deformation or tilting depends the extent of liquefaction, spatial variability of the soil, asymmetric mass and stiffness of the building, asymmetric loading from the ground motion and foundation type. Some of these parameters have been explored in Deliverable 3.2 (Viana da Fonseca et al., 2018), while a more comprehensive study on the parameters that influence tilt can be found in Bullock et al. (2018). The difference between global tilt and local deformation is strongly governed by the building's foundation type. In case of structures or infrastructure facilities with shallow foundations, the distinction will be whether these are rigid or flexible. Buildings resting on foundations that lack sufficient relative stiffness, compared to soft underlying soils, can experience either differential movements (i.e. differential lateral spreading or differential vertical settlements). In cases of buildings on flexible (i.e. unrestrained) foundations, columns and walls can move independently (either under lateral spreading or vertical settlements), and thus differentially, and damage occurs in the structural elements (**Figure 4.1**).



This project has received funding from the European Union's Horizon 2020 research and innovation programme under grant agreement No. 700748

Design guidelines for the application of soil characterisation and liquefaction risk assessment protocols

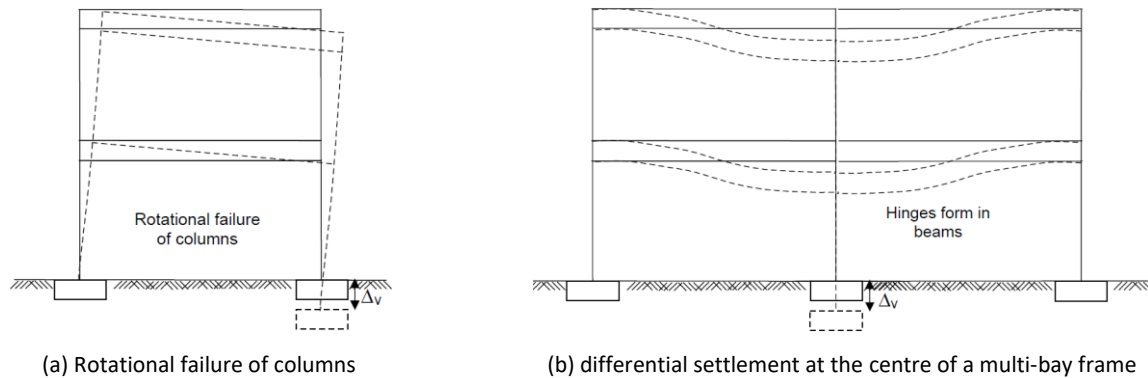


Figure 4.1. Behaviour of frame buildings with flexible shallow foundations due to differential vertical ground settlements (Bird et al. 2006).

For rigid foundation systems, the deformation is primarily uniform settlement of structure (**Figure 4.2a**) or global tilt (**Figure 4.2b**). The displacement is uniform and therefore does not result in damage to the superstructure.

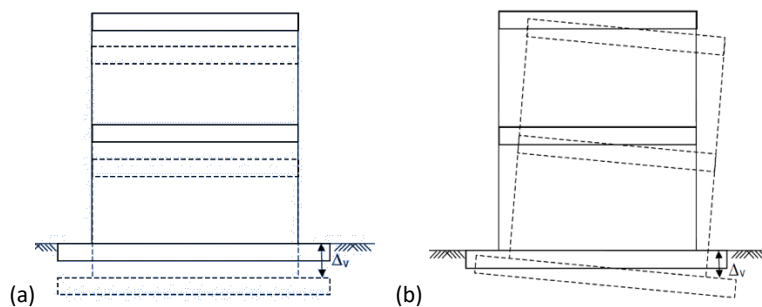


Figure 4.2. (a) Liquefaction-induced uniform vertical settlements of building with stiff shallow foundations; (b) differential vertical settlements of building (rotation) with stiff shallow foundations (Bird et al. 2006).

The parameters used to quantify the performance of a building are highlighted in **Figure 4.3**, and were divided into dynamic performance parameters and residual performance parameters. Dynamic performance parameters involve the shear force in the beams (V_{beam}) and columns (V_{column}), the chord rotation in the beams (θ_{beam}) and columns (θ_{column}) and the interstorey drift ($\theta_{ss,p}$). It is noted that, for columns, the exceedance of limit values of shear force or ultimate chord rotation was considered collapse, while for beams, the exceedance of limit values of shear force or ultimate chord rotation in a whole storey was considered collapse. For the interstorey drift, damage states were defined for thresholds of 0.5%, 1%, 2% and 3%, and above 3% while above 5% was considered collapse. Residual performance parameters involve maximum residual interstorey drift $\theta_{ss,r}$ and residual rotation of the foundation $\beta_{f,r}$ both at the local and global levels.



This project has received funding from the European Union's Horizon 2020 research and innovation programme under grant agreement No. 700748

Design guidelines for the application of soil characterisation and liquefaction risk

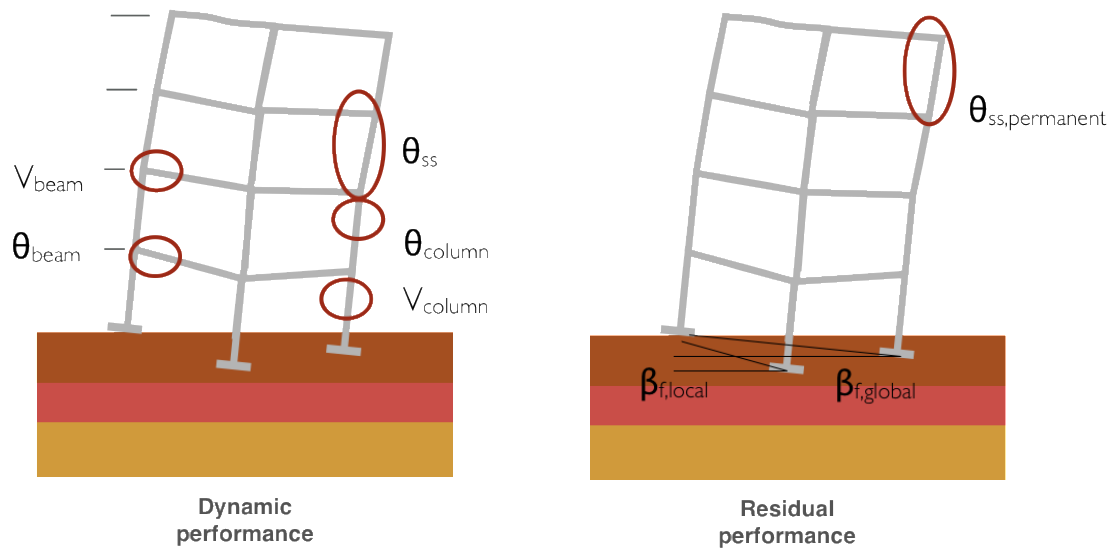


Figure 4.3: Dynamic performance parameters and residual performance parameters used to quantify the performance of a building.

4.2 METHODS TO QUANTIFY VULNERABILITY

The vulnerability assessment process requires the building performance to be evaluated against hazard intensity, typically with fragility curves or vulnerability curves. The hazard intensity is typically set using the ground motion intensity measures previously discussed, and the performance is obtained by simulating the building-soil system and calculating the performance criteria referred in the previous section (collapse, peak local response, peak and residual interstorey drift, and foundation tilt). Building damage and performance under liquefaction-induced ground deformations are a direct function of the properties of the structural system but also of the type of foundation. With respect to the former, the exposure model and the BCIM are expected to provide the necessary data for the simulations that need to be performed for a regional seismic risk and loss assessment. However, for the latter, detailed information is not expected to be available and will be very difficult to collect for a large portfolio of buildings. Therefore, assumptions need to be made and an adequate model for the uncertainty of the foundation system needs to be added to the BCIM model previously described. For a building-specific seismic risk and loss assessment, as referred before, it is expected that adequate and detailed information about the necessary characteristics of the building, including the foundation system, is available or can be obtained based on in situ surveys. Another viable option is to perform a simulated design of the building based on the design codes at the date of construction, this can be used to estimate unknown properties in the building as well as to size the foundation.

The assessment of vulnerability is directly tied to the classification used in the exposure model. The outlined exposure model considers building-soil classes to implicitly capture the soil-structure interaction (SSI) effects within the class. Compared to independent models of the soil and building that require some interaction function to account for the influence of SSI and to account for the combination of shaking and liquefaction induced damage. Since the building-soil system is part of a single class the system can be assessed either directly through modelling the soil and the building in a single numerical or experimental model or in a



This project has received funding from the European Union's Horizon 2020 research and innovation programme under grant agreement No. 700748

modular approach where different macro-mechanisms are first quantified and then connected through consideration of their interactions. The direct model is advantageous in that the interactions between all the mechanisms are implicitly accounted for. However, it is practically impossible to capture experimentally a detailed soil model and a detailed nonlinear structural model across a wide range of ground motions, even with a centrifuge, due to scaling laws and costs of experiments. Numerically, a direct model is possible although none of the widely used state-compatible constitutive models exist in any widely used software that also contains suitable constitutive models for structural modelling. Therefore, a trade-off must be made in reduced accuracy for the soil or structure. The direct approach is computationally demanding as stiff structural elements often require a very small time step, while the large soil domain means there are many elements to be assessed at each time step. Also, a direct approach does not benefit from generalising behaviour, in that a change in one assumption would require the numerical model to be completely re-run. In the case of embankments where the entire model is soil, then these drawbacks have a minimal impact, and the procedure outlined for vulnerability assessment of embankments in Deliverable 3.2 (Viana da Fonseca et al., 2018), successfully uses the direct modelling approach.

The alternative approach that was adopted for the performance of buildings was the macro-mechanism approach. The macro-mechanism approach captures the macro behaviour of the soil profile and building using submodels (e.g. pore pressure model, settlement model), and explicitly accounts for their interaction. The main advantages of this approach are that it is numerical efficient, can include multiple different methods at each modular step, can evaluate the uncertainties at each step. The full details of the macro-mechanism approach is described and applied to a case study building in Part 2 of Deliverable 3.2 (Viana da Fonseca et al., 2018).

4.3 DISCUSSION OF THE ROLE OF VULNERABILITY FUNCTIONS

In seismic risk and loss assessment studies, a vulnerability function is a mathematical model that expresses building loss, often in terms of a ratio of cost of repair to cost of replacement, as a function of a ground motion intensity measure (IM) that represents earthquake severity. Furthermore, this IM is usually selected to be the same (or at least compatible) with the parameter that is used to represent earthquake hazard.

Traditionally, in seismic risk and loss assessment studies, analytical vulnerability functions (i.e. those based on the numerical simulation of building models subjected earthquake loading) can be obtained using one of two approaches (see Viana da Fonseca et al., 2017) for details and references cited therein). One of the approaches involves the simulation of analytical fragility functions for multiple performance levels that are then combined with consequence functions that express the expected level of loss for a given performance level. However, currently, there is no consequence model explicitly accounting for liquefaction-induced damage available in the literature. The second approach involves a procedure that derives storey-level vulnerability functions. The vulnerability functions obtained by this approach express the repair cost of components on a given storey as a function of storey-level demand (interstorey drift, peak floor acceleration, or other measures of storey-level structural response). Although this approach was not originally developed to account for liquefaction-induced losses, it was deemed easier to adapt it to include this additional loss component. Nevertheless, it should be noted that adapting both approaches to account for liquefaction-



This project has received funding from the European Union's Horizon 2020 research and innovation programme under grant agreement No. 700748

induced losses involves a considerable level of uncertainty. Even though the building's structural response due to liquefaction-induced deformations can be quantified with an adequate level of reliability, determining structural and non-structural performance, and consequently repair costs and losses, based on those response parameters is still subjective and relies essentially on expert opinion due to insufficient data.

The procedure developed in LIQUEFACT D3.2 report is briefly outlined below in **Figure 4.4**. The first step is the classification of the building-soil class. For the selected class either a single building and soil profile is analysed, or if some of the parameters of the building or soil profile are unknown then a population of representative buildings and soil profiles should be developed based on the selected building-soil class. The macro-mechanism approach then considers a upward propagating ground motion and quantifies the time of liquefaction (Step 2) and the modification due to liquefaction on the surface ground motion, soil-foundation stiffness, and settlement (Steps 3-5 respectively). The results of steps 3-5 are used as inputs into the seismic analysis of the building (Step 6), the process is repeated for different instances of the building-soil class and for different ground motions and the performance is measured in terms of peak interstorey drift, residual interstorey drift, foundation tilt, and collapse (Step 7). The results of step 7 are aggregated to develop fragility curves (Step 8) which are then combined to compute the expected loss.

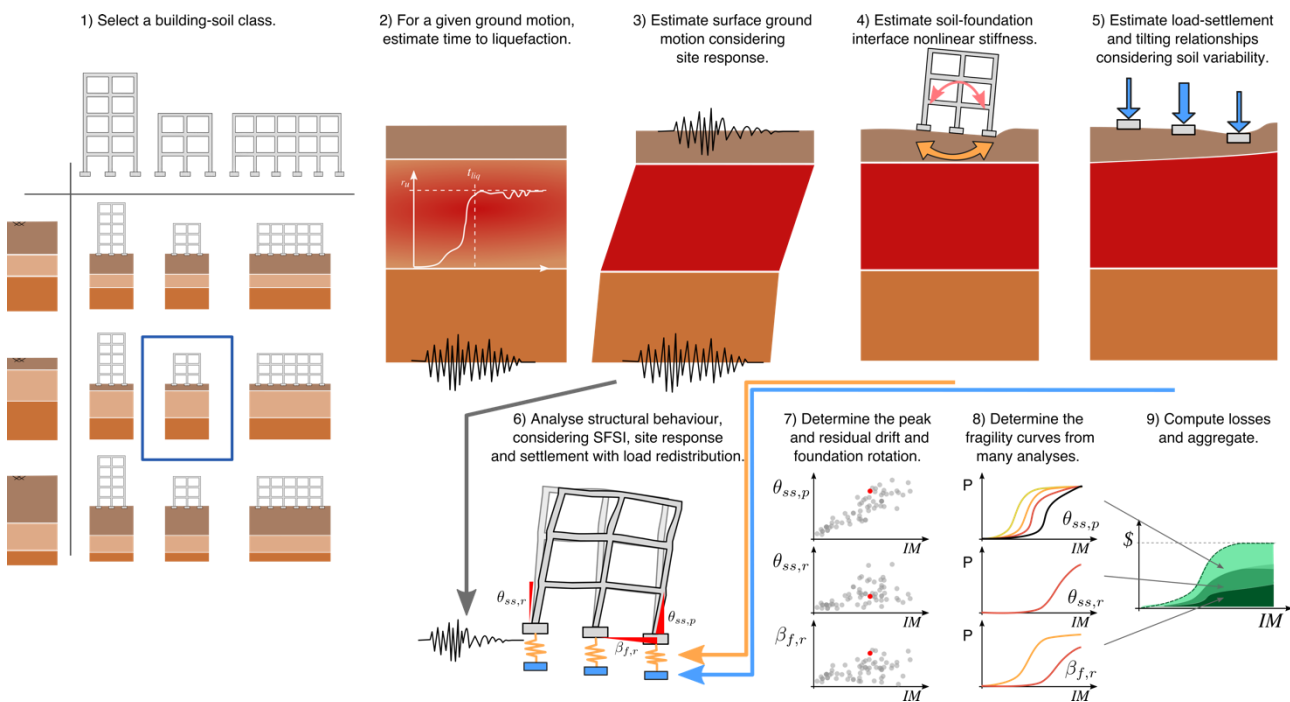


Figure 4.4: Application of the macro-mechanism approach to assess vulnerability and losses

REFERENCES

Bird, J.F., Bommer, J.J., Crowley, H. and Pinho, R. (2006) Modelling liquefaction-induced building damage in earthquake loss estimation. *Soil Dynamics and Earthquake Engineering* 26(1), 15–30.



This project has received funding from the European Union's Horizon 2020 research and innovation programme under grant agreement No. 700748

- Bullock, Z., Dashti, S., Karimi, Z., Liel, A., Porter, K. and Franke, K. (2019). "Probabilistic Models for the Residual and Peak Transient Tilt of Mat-Founded Structures on Liquefiable Soils," ASCE Journal of Geotechnical and GeoEnvironmental Engineering, 145(2).
- Viana da Fonseca, A., Millen, M., Gómez-Martinez, F., Romão, X., Quintero, J., Gómez, F., Costa, P., Rios, S., Kosič, M., Dolšek, M., Logar, J., Oztoprak, S., Bozbey, I., Kelesoglu, K., Ozcep, F., Flora, A., Rasulo, A., Modoni, G. and Croce, P. (2017) State of the art review of numerical modelling strategies to simulate liquefaction-induced structural damage and of uncertain/random factors on the behaviour of liquefiable soils. DELIVERABLE 3.1 of LIQUEFACT project "Assessment and mitigation of liquefaction potential across Europe: a holistic approach to protect structures / infrastructures for improved resilience to earthquake-induced liquefaction disasters" (www.liquefact.eu)
- Viana da Fonseca, A., Millen, M., Romão, X., Quintero, J., Rios, S., Ferreira, C., Panico, F., Azeredo, C., Pereira, N., Logar, J., Oblak, A., Dolšek, M., Kosič, M., Kuder, S., Logar, M., Oztoprak, S., Kelesoglu, M. K., Sargin, S., Oser, C., Bozbey, I., Flora, A., Billota, E., Prota, A., Di Ludovico, M., Chiaradonna, A., Modoni, G., Paoella, L., Spacagna, R., Lai, C.G., Shinde, S. and Bozzoni, F. (2018). Methodology for the liquefaction fragility analysis of critical structures and infrastructures: description and case studies. DELIVERABLE 3.2 of LIQUEFACT project "Assessment and mitigation of liquefaction potential across Europe: a holistic approach to protect structures / infrastructures for improved resilience to earthquake-induced liquefaction disasters" (www.liquefact.eu)



This project has received funding from the European Union's Horizon 2020 research and innovation programme under grant agreement No. 700748

5. COMPUTATION OF LOSSES

Typical seismic risk and loss assessment studies have been quantifying risk and losses according to the well known Pacific Earthquake Engineering Research Centre (PEER) methodology or according to variations of this approach that can be obtained by aggregating some of the steps (e.g. see Ramirez and Miranda (2009) for additional background when a storey-based approach is used to define vulnerability functions). The PEER methodology was developed to answer the need for communicating seismic risk to stakeholders involving metrics that reflect seismic consequences and are different than the engineering terms usually adopted in earthquake engineering. This methodology allows for the quantification, in probabilistic terms, of different decision variables (DVs) such as monetary losses, repair time or number of fatalities. The basis of the PEER methodology lies in the probabilistic characterization of several performance metrics along with the multiple sources of uncertainty that are inherent to seismic assessment (e.g. the uncertainty about the hazard, the ground motions representing a seismic scenario, the modelling and knowledge-based uncertainties of the building components and properties). The PEER methodology can be summarized into the framing equation representing the rate of a certain DV exceeding a value dv (Cornell and Krawinkler, 2000):

$$\lambda(DV > dv) = \int \int \int_{IMEDPDM} G(DV|DM) \cdot |dG(DM|EDP)| \cdot |dG(EDP|IM)| \cdot |d\lambda(IM)| \quad (5.1)$$

where DM represents a damage measure, generally discretised into several damage states, EDP represents measure of the structural response that can be correlated with DM, IM is a ground motion intensity measure and $G(\cdot)$ is the complementary cumulative distribution function. The numerical integration of **Equation (5.1)** can be used to estimate the annual losses. A discrete solution of **Equation (5.1)** requires the quantification of the expected loss value, $E(L|IM_i)$, for each ground motion intensity IM_i , and, for the case where liquefaction-induced damage is not accounted for, can be estimated from the proposal of Ramirez and Miranda (2009), based on previous work by Aslani (2005):

$$E(L|IM_i) = E(L|\bar{C} \cap R, IM_i) \cdot p(\bar{C} \cap R|IM_i) + E(L|\bar{C} \cap D, IM_i) \cdot p(\bar{C} \cap D|IM_i) + E(L|C, IM_i) \cdot p(C|IM_i) \quad (5.2)$$

where $E(L|\bar{C} \cap R, IM_i)$, $E(L|\bar{C} \cap D, IM_i)$ and $E(L|C, IM_i)$ are the expected value of the losses for IM_i given that the structure is still reparable (without collapsing), the expected value of the losses for IM_i given that the structure is not reparable (without collapsing) and the expected value of the losses for IM_i given that the structure will collapse, respectively.

The event representing the case where the building did not collapse and is reparable $\bar{C} \cap R$ corresponds to:



This project has received funding from the European Union's Horizon 2020 research and innovation programme under grant agreement No. 700748

$$\begin{aligned} \bar{C} \cap R = & \bigcap_{j=1}^{m \text{ columns}} \left(\frac{V_j}{V_{\max,j}} \leq 1 \right) \cap \bigcap_{j=1}^{m \text{ columns}} \left(\frac{\theta_j}{\theta_{\max,j}} \leq 1 \right) \cap \bigcap_{i=1}^{n \text{ storeys}} \max \left(\frac{V_j}{V_{\max,j}} \bigg|_{j=1,m \text{ beams}} \right) \leq 1 \\ & \cap \bigcap_{i=1}^{n \text{ storeys}} \max \left(\frac{\theta_j}{\theta_{\max,j}} \bigg|_{j=1,m \text{ beams}} \right) \leq 1 \cap \bigcap_{i=1}^{n \text{ storeys}} \max \left(\frac{\theta_{ss,p,j}}{\theta_{ss,p,\max}} \right) \leq 1 \cap \bigcap_{i=1}^{n \text{ storeys}} \max \left(\frac{\theta_{ss,r,j}}{\theta_{ss,r,\max}} \right) \leq 1 \end{aligned} \quad (5.3)$$

and represents the occurrence of damage states where the interstorey drift $\theta_{ss,p}$ reaches thresholds $\theta_{ss,c}$ of 0.5%, 1%, 2% and 3%. Therefore:

$$p(\bar{C} \cap R | IM_i) = p\left(\max(\theta_{ss,p,j})_{j=1,n \text{ storeys}} = \theta_{ss,c} | IM_i\right) \quad (5.4)$$

However, the probabilities of having a repairable (R) and an irreparable (D) building without collapsing, $p(\bar{C} \cap R | IM_i)$ and $p(\bar{C} \cap D | IM_i)$, respectively, can be calculated by factorizing the corresponding probability of demolition $p(D | \bar{C}, IM_i)$ by the probability of collapse, $p(C | IM_i)$.

Finally, the expected value of the losses for a given ground motion intensity IM_i can be quantified considering a relative quantity, the loss ratio, defined by the ratio between the obtained losses and the cost of replacing the structure. This implies that the loss ratio is 1.0 when the structure is considered irreparable or when structural collapse is observed, and **Equation (5.2)** becomes:

$$\begin{aligned} E(L | IM_i) = & E(L | \bar{C} \cap R, IM_i) \cdot [1 - p(D | \bar{C}, IM_i)] \cdot [1 - p(C | IM_i)] + \\ & + p(D | \bar{C}, IM_i) \cdot [1 - p(C | IM_i)] + p(C | IM_i) \end{aligned} \quad (5.5)$$

If a loss ratio larger than 1.0 needs to be considered for the case where the structure is considered irreparable, **Equation (5.5)** can be defined instead by:

$$\begin{aligned} E(L | IM_i) = & E(L | \bar{C} \cap R, IM_i) \cdot [1 - p(D | \bar{C}, IM_i)] \cdot [1 - p(C | IM_i)] + \\ & + p(D | \bar{C}, IM_i) \cdot [1 - p(C | IM_i)] \cdot DRC + p(C | IM_i) \end{aligned} \quad (5.6)$$

where factor DRC now represents the ratio between the demolition and reconstruction cost as a function of the cost of constructing a new building.

In order to account for damage scenarios involving a combined building-foundation damage state, the event corresponding to the case where the building did not collapse and is repairable $\bar{C} \cap R$ is now considered to involve the occurrence of a given building damage level and a given foundation damage level. Therefore, **Equation (5.3)** now becomes:



This project has received funding from the European Union's Horizon 2020 research and innovation programme under grant agreement No. 700748

$$\begin{aligned} \bar{C} \cap R = & \bigcap_{j=1}^{m \text{ columns}} \left(\frac{V_j}{V_{\max,j}} \leq 1 \right) \cap \bigcap_{j=1}^{m \text{ columns}} \left(\frac{\theta_j}{\theta_{\max,j}} \leq 1 \right) \cap \bigcap_{i=1}^{n \text{ storeys}} \max \left(\frac{V_j}{V_{\max,j}} \bigg|_{j=1,m \text{ beams}} \right) \leq 1 \\ & \cap \bigcap_{i=1}^{n \text{ storeys}} \max \left(\frac{\theta_j}{\theta_{\max,j}} \bigg|_{j=1,m \text{ beams}} \right) \leq 1 \cap \bigcap_{i=1}^{n \text{ storeys}} \max \left(\frac{\theta_{ss,p,j}}{\theta_{ss,p \max}} \right) \leq 1 \cap \bigcap_{i=1}^{n \text{ storeys}} \max \left(\frac{\theta_{ss,r,j}}{\theta_{ss,r \max}} \right) \leq 1 \cap \bigcap_{i=1}^k \max \left(\frac{\beta_{f,j}}{\beta_{f,r}} \right) \leq 1 \end{aligned} \quad (5.7)$$

where β_f is the rotation of the foundation and $\beta_{f,r}$ is the residual rotation of the foundation. Consequently, **Equation (5.4)** becomes:

$$p(\bar{C} \cap R | IM_i) = p\left(\max(\theta_{ss,p,j})_{j=1,n \text{ storeys}} = \theta_{ss,c} | IM_i\right) \times p\left(\max(\beta_{f,j})_{j=1,n \text{ foundations}} = \beta_{f,c} | IM_i\right) \quad (5.8)$$

by assuming that the occurrence of a given building damage level and a given foundation damage level defined by a certain threshold $\beta_{f,c}$ are independent (though not entirely true, as a strong motion would typically damage the building and results in large settlement, see discussion in intensity measures in Section 3 above). For this combined building-foundation damage state, the expected value of the losses given that the structure is still reparable (without collapsing) $E(L | \bar{C} \cap R, IM_i)$ was considered to be defined by:

$$E(L | \bar{C} \cap R, IM_i) = p(\bar{C} \cap R | IM_i) \times L(\theta_{ss,p} + \beta_f) \quad (5.9)$$

where the loss factor $L(\theta_{ss,p} + \beta_f)$ is defined by:

$$L(\theta_{ss,p} + \beta_f) = \min\left(E\left(L | \max(\theta_{ss,p,j})_{j=1,n \text{ storeys}} = \theta_{ss,c}, IM_i\right) + E\left(L | \max(\beta_{f,j})_{j=1,n \text{ foundations}} = \beta_{f,c}, IM_i\right), DRC\right) \quad (5.10)$$

which amounts to saying that the expected value of the losses for a combined building-foundation damage state is the sum of the expected losses from the reparable building damage with the expected losses from the foundation damage, but always less than or equal to the demolition and reconstruction cost (represented by the factor DCR), since they are assumed independent, factored by the probability of occurrence of the combined damage state. It noted that the value of **Equation (5.9)** obtained by evaluating all the relevant building damage levels and foundation damage levels and summing the values obtained for the damage state combinations. Following these changes to account for damage scenarios involving a combined building-foundation damage state, the expected value of the losses for a given ground motion intensity IM_i can be quantified according to **Equation (5.6)**.

Quantifying the expected value of the losses for a given ground motion intensity IM_i according to **Equation (5.6)** requires the calculation of $p(D | \bar{C}, IM_i)$, $p(C | IM_i)$ and $p(\bar{C} \cap R | IM_i)$ defined by **Equation (5.8)**. These quantities are directly obtained based on the statistical post-processing of the results of nonlinear dynamic analyses of the structure (e.g. using counted data or by fitting fragility curves for each damage state).



This project has received funding from the European Union's Horizon 2020 research and innovation programme under grant agreement No. 700748

Design guidelines for the application of soil characterisation and liquefaction risk

On the other hand, the terms $L | \max(\theta_{ss,pj})_{j=1,n \text{ storeys}} = \theta_{ss,c}$ and $L | \max(\beta_{fj})_{j=1,n \text{ foundations}} = \beta_{f,c}$ require the definition of loss curves; the former a loss curve defining the expected loss for increasing levels of interstorey drift and the former a loss curve defining the expected loss for increasing levels of foundation rotation. While loss curves defining the expected loss for increasing levels of interstorey drift can be obtained based on expected component loss levels (e.g. see (Ramirez and Miranda, 2009) and more recently (Papadopoulos et al., 2018)), no approach has been defined so far to define loss curves defining the expected loss for increasing levels of foundation rotation. Furthermore, there is limited information available on foundation repair costs and the possibility of repairing the building foundations is also significantly dependent on the market. Therefore, for the purpose of the research presented herein, it has been assumed here that the market is willing to accept a repair cost of 30% of the total cost of the building, and that repair techniques would be available to meet the market demand.

5.1. LOSS CALCULATION EXAMPLE CASE STUDY

Following the vulnerability procedure outlined in D3.2, it is assumed that the following fragility curves were developed for an intensity measure of spectral acceleration at one second (**Figure 5.1**). The loss calculations are demonstrated for a spectral acceleration of 0.57s.

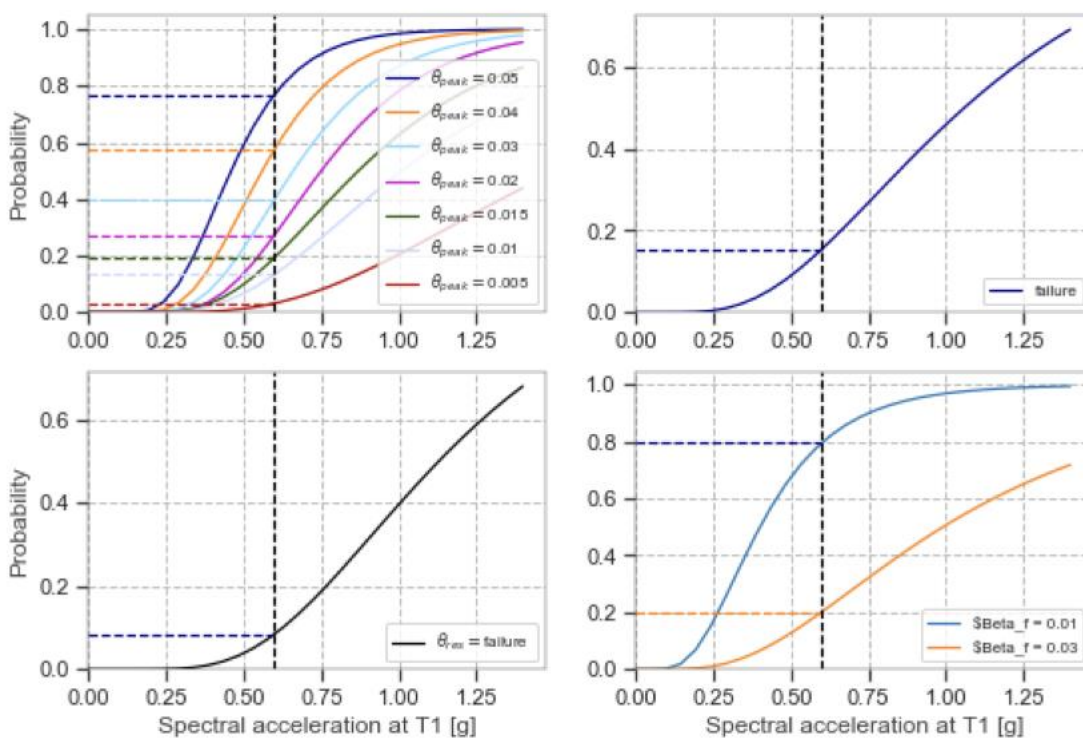


Figure 5.1: Obtaining probabilities from fragility curves

The building can be assumed to have the following building, foundation and combined performance damage states (**Table 5.1**, **Table 5.2** and **Table 5.3**) and associated losses and probabilities (from the fragility curves).



This project has received funding from the European Union's Horizon 2020 research and innovation programme under grant agreement No. 700748

Design guidelines for the application of soil characterisation and liquefaction risk assessment protocols

The building losses are based on tables of losses vs peak drift for different number of storeys, building types and building uses from research by Ramirez, C. M., & Miranda, E. (2009). However, in the original research the drift was de-aggregated into drift sensitive and floor acceleration sensitive components. If no floor acceleration data is available then the floor acceleration sensitive data will be merged with the non-structural drift sensitive components. The merge floor ensures that the sum of losses equals 1 at drift of 5%.

In this example values are taken from page B-20 of Ramirez, C. M., & Miranda, E. (2009) and no floor accelerations were considered so values are merged.

Table 5.1: Building damage states and associated losses and probabilities

Damage state	Loss %	Probability
BD_DS1	0	0.1
BD_DS2	0.1	0.15
BD_DS3	0.2	0.15
BD_DS4	0.35	0.1
BD_DS5	0.5	0.1
BD_DS6	0.7	0.1
BD_DS7	0.9	0.15
BD_DS8	1.0	0.15
Total		1

Table 5.2: Foundation damage states and associated losses and probabilities

Damage state	Loss %	Probability
FD_DS1	0	0.4
FD_DS2	0.3	0.3
FD_DS3	1.0	0.3
Total		1

Table 5.3: Combine performance damage states and associated losses and probabilities



This project has received funding from the European Union's Horizon 2020 research and innovation programme under grant agreement No. 700748

Damage state	Loss %	Probability
Residual drift limit	100	0.7
Collapse	100	0.4

The combine damage for each of the building-foundation damage states is produced in **Table 5.4(Equation (5.11))**, ensuring that the sum of the damage does not exceed the demolition and replace cost (L_{demo}), in this case it is set to 1.0.

$$L [DS_{IDR_i} \cap DS_{FD_j}] = \min (L[DS_{IDR_i}] + L [DS_{FD_j}], L_{demo}) \quad (5.11)$$

Table 5.4: Combined building foundation damage states

	FD_DS1	FD_DS2	FD_DS2
BD_DS1	0	0.3	1
BD_DS2	0.1	0.4	1
BD_DS3	0.2	0.5	1
BD_DS4	0.35	0.65	1
BD_DS5	0.5	0.8	1
BD_DS6	0.7	1	1
BD_DS7	0.9	1	1
BD_DS8	1	1	1

The probability of each building-foundation damage state is computed in **Table 5.5 (Equation (5.12))**.

$$P [DS_{IDR_i} \cap DS_{FD_j}] = P[DS_{IDR_i}] \cdot P [DS_{FD_j}] \quad (5.12)$$

Table 5.5: Probabilities of each building-foundation damage state



This project has received funding from the European Union's Horizon 2020 research and innovation programme under grant agreement No. 700748

	FD_DS1	FD_DS2	FD_DS2
BD_DS1	0.07	0.03	0.03
BD_DS2	0.105	0.045	0.045
BD_DS3	0.105	0.045	0.045
BD_DS4	0.07	0.03	0.03
BD_DS5	0.07	0.03	0.03
BD_DS6	0.07	0.03	0.03
BD_DS7	0.105	0.045	0.045
BD_DS8	0.105	0.045	0.045

The losses associated to each building-soil damage state are calculated in **Table 5.6(Equation (5.13))** and the sum of the losses (unconditioned on the combined performance damage states) (i.e. sum of values in **Table 5.5)** was equal to 0.85.

$$L_{damage} = \sum_{i=0}^{i=n} \sum_{j=0}^{j=n} P [DS_{IDR_i} \cap DS_{FD_j}] \cdot L [DS_{IDR_i} \cap DS_{FD_j}] \quad (5.13)$$

Table 5.6: Losses associated to each building-soil damage state

	FD_DS1	FD_DS2	FD_DS2
BD_DS1	0	0.009	0.03
BD_DS2	0.0105	0.018	0.045
BD_DS3	0.021	0.0225	0.045
BD_DS4	0.0245	0.0195	0.03
BD_DS5	0.035	0.024	0.03
BD_DS6	0.049	0.03	0.03
BD_DS7	0.0945	0.045	0.045
BD_DS8	0.105	0.045	0.045

Finally, the total loss (L_{total}) associated to this hazard level are calculated using **Equations (5.14)** and **(5.15)** by considering the combined performance probabilities (collapse and residual drift), where the total loss was 87%.



This project has received funding from the European Union's Horizon 2020 research and innovation programme under grant agreement No. 700748

$$L_{total} = L_{damage}(1 - P_{demo})(1 - P_{collapse}) + L_{demo}P_{demo}(1 - P_{collapse}) + L_{collapse}P_{collapse} \quad (5.14)$$

$$L_{total} = 0.85(1 - 0.07)(1 - 0.04) + 1.0 \cdot 0.07(1 - 0.04) + 1.0 \cdot 0.04 = 0.87 \quad (5.15)$$

REFERENCES

- Aslani, H. (2005) Probabilistic earthquake loss estimation and loss disaggregation in buildings. PhD Dissertation. Stanford University.
- Cornell C.A. and Krawinkler H (2000). Progress and challenges in seismic performance assessment, PEER Centre News 3(2):1-3.
- Papadopoulos, A. N., Vamvatsikos, D. and Kazantzi, A. K. (2018) Development and application of FEMA P-58 compatible story loss functions. Earthquake Spectra, doi: /10.1193/102417EQS222M.
- Ramirez, C. and Miranda, E. (2009) Building-specific loss estimation methods and tools for simplified performance based earthquake engineering. Report N° 171. John A. Blume earthquake engineering research center. Stanford University. Stanford, California, USA.



This project has received funding from the European Union's Horizon 2020 research and innovation programme under grant agreement No. 700748

6. FINAL REMARKS

This report provided an overview of the key steps for assessing the risk of infrastructures that are exposed to liquefaction. Key aspects related to the definition of exposure models in a situation where liquefaction effects may be relevant was discussed and an equivalent soil profile scheme for classifying liquefaction susceptibility was analysed. This classification scheme should then be combined with existing infrastructure taxonomies for the purpose of developing a combined exposure model accounting for liquefaction susceptibility. Other important aspects relevant to the topic of ground motion selection for earthquake loss assessment were discussed, namely addressing the issues around multiple ground motion intensities measures in soil-liquefaction-foundation-structure interaction problems. Given the differences in the relevant intensity measures depending on the type of damage under consideration (structural damage is typically best correlated to peak energy based intensity measures, while liquefaction is more strongly correlated to cumulative energy-based intensity measures), an approach that would be able to account for the information associated to both types of intensity measures was also discussed. Finally, reference is made to the novel procedure presented for the calculation of losses accounting for liquefaction-induced ground deformations that is based on a state-of-the-art approach for calculating infrastructure losses probabilistic seismic loss assessment. The information that is needed to implement such procedure is discussed, highlighting current limitations of available data and a case study loss example calculation is presented that demonstrates the applicability of the procedure.